A GENERAL FORMULATION OF COMBUSTION INSTABILITY FOR RAMJETS AND AFTERBURNERS

Hyun-Gull Yoon

Agency for Defense Development
4-4-1, Yuseong P.O.Box 35-4, Taejeon, Korea

ABSTRACT

A wave equation and a comprehensive linear combustion model are developed for ramjet and afterburner combustion instability predictions. Modal analysis is used to develop general results for frequencies and damping factors and examples of their applications are given.

1. Introduction

In the development of ramjet and afterburner combustion systems, one of the major concerns is the creation of large amplitude pressure oscillations by unsteady combustion. These self-excited oscillations (referred to as combustion instabilities) are driven by a coupling between the unsteady heat release and an acoustic oscillation at one of the resonant modes of the system. Such oscillations, accompanied by excessive vibrations and heat transfer to the combustor walls, can cause system failure in extreme cases.

Low frequency oscillations in the range of 50-500 Hz and generally characterized by longitudinal modes at the resonant frequencies of the combustor seem to be the most important in ramjet and afterburner combustion chambers. Several investigators such as Culick (1988), Langhorne (1988), Bloxsidge, Dowling, and Langhorne (1988), and Shyy and Udaykumar (1990) have suggested that these instabilities are primarily velocity sensitive. Velocity sensitive combustion instability is, therefore, the subject of this paper.

2. Governing Equations

Consider a combustion chamber in the form of a duct of length L having an inlet at the left end. The combustion chamber contains a flowing mixture of fuel, oxidizer, and products of combustion which will be treated herein as an inviscid nonconducting ideal gas with gas constant R and ratio of specific heats γ. Treating the flow as one-dimensional, the respective conservation equations for mass, linear momentum, and total energy are

$$\frac{\partial \rho}{\partial t} + \rho\frac{\partial u}{\partial x} + u\frac{\partial \rho}{\partial x} = 0$$

$$\rho\left(\frac{\partial u}{\partial t} + u\frac{\partial u}{\partial x}\right) = -\frac{\partial p}{\partial x} + D \tag{1}$$

$$\frac{\partial}{\partial t}\left[\rho\left(e + \frac{u^2}{2}\right)\right] + \frac{\partial}{\partial x}\left[u\rho\left(e + \frac{u^2}{2}\right) + up\right] = Q$$

where x is axial position, t is time, ρ is density, u is axial velocity, p is pressure, D is axial body force per unit volume, e is specific internal energy, and Q is the heat addition rate per unit volume. The equations of state are

$$p = \rho RT, \qquad e = \frac{RT}{\gamma-1} \tag{2}$$

It is convenient to introduce dimensionless quantities by the following transformations

$$x \rightarrow Lx, \qquad t \rightarrow \frac{L}{c_i}t, \qquad \rho \rightarrow \rho_i(1+\bar{\rho}+\rho), \qquad u \rightarrow c_i\left(u_0+\bar{\phi}'+\frac{\partial\phi}{\partial x}\right),$$
$$p \rightarrow \frac{\rho_i c_i^2}{\gamma}(1+\bar{p}+p), \quad T \rightarrow \frac{c_i^2}{\gamma R}(1+\bar{T}+T), \quad D \rightarrow \frac{\rho_i c_i^2}{L}\left(\bar{A}'+\frac{\partial A}{\partial x}\right), \quad Q \rightarrow \frac{\rho_i c_i^3}{L}(\bar{Q}+Q) \tag{3}$$

where the symbol $\rightarrow$ indicates a transition from dimensional quantities (tail) to corresponding dimensionless quantities (tip), a bar indicates a steady state quantity (function of x only), a prime indicates differentiation of a function of one variable with respect to its argument, ρ_i is the initial density, c_i is the initial sound speed, u_0 is the dimensionless inlet velocity, ϕ denotes velocity potential, and A denotes force potential. The dimensionless dependent variables are treated as small perturbations from a reference state characterized by unit pressure, temperature, density, and constant velocity u_0. Terms that are linear in the perturbations will be called first order terms, those quadratic in the perturbations second order terms, etc. It is desired to obtain a system of equations structured such that the first order terms will be those associated with the equations of linear acoustics and all additional effects (body force, heat addition, mean flow, nonlinearity) will appear as second order corrections. (This approach is similar to that of Culick (1988) and is motivated by observations that the disturbances associated with combustion instabilities usually closely resemble the acoustic modes of the chamber.) Toward this end u_0 will be treated as a first order term while the sources will be treated as second order terms. Substituting (3) into (1) and (2), retaining only first and second order terms, and carrying out a number of manipulations (omitted for the sake of brevity) yields

$$\bar{u} = \bar{\phi}' = (\gamma-1)\int_0^x \bar{Q}(\xi)\,d\xi, \qquad \bar{T} = -\bar{\rho} = \frac{\bar{u}}{u_0}, \qquad \bar{p} = 0 \tag{4}$$

for the steady state solution (assuming $\bar{A} = 0$) and

$$\frac{\partial^2\phi}{\partial t^2} - \frac{\partial^2\phi}{\partial x^2} + 2u_0\frac{\partial^2\phi}{\partial x\partial t} + 2\frac{\partial\phi}{\partial x}\frac{\partial^2\phi}{\partial x\partial t} + (\gamma-1)\frac{\partial\phi}{\partial t}\frac{\partial^2\phi}{\partial x^2} - \frac{\partial A}{\partial t} + (\gamma-1)Q = 0$$

$$\rho = -\frac{\partial\phi}{\partial t} - u_0\frac{\partial\phi}{\partial x} - \frac{1}{2}\left(\frac{\partial\phi}{\partial x}\right)^2 - \frac{(\gamma-2)}{2}\left(\frac{\partial\phi}{\partial t}\right)^2 + A - (\gamma-1)\int_0^t Q(x,\eta)\,d\eta \tag{5}$$

$$T = (\gamma-1)\left[-\frac{\partial\phi}{\partial t} - u_0\frac{\partial\phi}{\partial x} - \frac{1}{2}\left(\frac{\partial\phi}{\partial x}\right)^2 + A\right] + (\gamma-1)\int_0^t Q(x,\eta)\,d\eta$$

$$p = \gamma\left[-\frac{\partial\phi}{\partial t} - u_0\frac{\partial\phi}{\partial x} + \frac{1}{2}\left(\frac{\partial\phi}{\partial t}\right)^2 - \frac{1}{2}\left(\frac{\partial\phi}{\partial x}\right)^2 + A\right]$$

for the stability problem. In (4) and (5) ξ and η are dummy variables. Since Q is a second order term according to the original assumptions, $\bar{u}$ is predicted to be a second order term (rather than first order as originally assumed) while $\bar{\rho}$ and T are predicted to be first order terms.

In the present work the heat addition term Q will be used to account for the burning process and the body force term A will be used to approximately represent the ability of devices such as baffles and liners to modify the frequency and damping characteristics of the system. These latter effects cannot be handled exactly in a one-dimensional formulation.

3. Linear Combustion Model

Several investigators such as Culick (1988), Langhorne (1988), Bloxsidge, Dowling, and Langhorne (1988), and Shyy and Udaykumar (1990) have suggested that the main features of the unsteady heat addition occurring in ramjets and afterburners can be modeled by treating the unsteady combustion as a linear velocity sensitive process. In this section, a general linear velocity sensitive combustion model will be developed which includes and generalizes the work of the above-mentioned authors.

The unsteady heating rate Q will be assumed to be proportional to the steady heating rate, i.e.,

$$Q(x,t) = \bar{Q}(x)\, q(x,t) \tag{6}$$

where $q(x,t)$ characterizes the unsteady heating response. Two different methods of modeling q are considered. These will be called the local model and the convection model. Each is discussed below.

The first model to be discussed will be called the local model herein. It assumes that the unsteady heating response at any point is a function of the unsteady velocity at that point and is characterized by the general equation

$$\mathcal{L}_1(q) = Y(t)\, \mathcal{L}_2(u) \tag{7}$$

where $\mathcal{L}_1$ and $\mathcal{L}_2$ are linear temporal operators and Y is an amplification factor which measures the influence of velocity perturbations on heating rate perturbations at any time.

Equation (7) is quite general and allows for a variety of responses. It is a time domain relation. An equivalent frequency domain relation can be obtained for the important special case in which Y is treated as a constant. This is done by substituting the harmonic functions

$$q(x,t) = \check{q}(x)e^{i\omega t}, \qquad u(x,t) = \check{u}(x)e^{i\omega t} \tag{8}$$

into (7) to obtain

$$\check{q} = Y I(\omega)\check{u}\ ; \qquad I(\omega) = I_R(\omega) + i\, I_I(\omega) \tag{9}$$

where the complex number $I(\omega)$ is an impedance function, the form of which depends on the forms of $\mathcal{L}_1$ and $\mathcal{L}_2$. In many situations information about $I(\omega)$ is supplied directly without a knowledge of $\mathcal{L}_1$ and $\mathcal{L}_2$.

The second model to be discussed will be called the convection model herein. It makes use of the equations

$$\frac{\partial q}{\partial t} + v_c(x,t)\frac{\partial q}{\partial x} = 0, \qquad q(x_s,t) = q_s(t) \tag{10}$$

where v_c is a convection velocity, x_s is the location of a heat source, and $q_s(t)$ characterizes the unsteady heating response at the source. According to this model, heating response perturbations originate at x_s and travel downstream with velocity v_c. The local flow velocity, the speed of sound, and the velocity of moving vortices have all been suggested as appropriate convection velocities. The problem defined by (10) has the general solution

$$q(x,t) = q_s(\theta)H(x-x_s) \tag{11}$$

with the relationship between θ, x, and t determined from solving the problem

$$\frac{dt}{dx} = \frac{1}{v_c}, \qquad t(x_s) = \theta \tag{12}$$

In the present work it will be assumed, for simplicity, that v_c is constant. Then (11) reduces to

$$q(x,t) = q_s(t-\frac{x-x_s}{v_c})H(x-x_s) \tag{13}$$

In a manner similar to (7), the relation between $q_s(t)$ and $u_s(t)=u(x_s,t)$ will be assumed to have the time domain form

$$\mathcal{L}_1(q_s) = Y(t)\mathcal{L}_2(u_s) \tag{14}$$

To obtain the equivalent frequency domain relationship for constant Y, one substitutes

$$q_s(t) = \check{q}_s e^{i\omega t}, \qquad u_s(t) = \check{u}_s e^{i\omega t} \tag{15}$$

into (14) which yields

$$\check{q}_s = YI(\omega)\check{u}_s \tag{16}$$

Substituting (8) and (15) into (13) and using (16) yields

$$\check{q} = YI(\omega)\check{u}_s e^{-i\omega(\frac{x-x_s}{v_c})} \tag{17}$$

Equation (17) has the same form as (9) with the addition of an exponential space shift factor. It can be shown that the convection model proposed herein includes the combustion response models employed by Culick (1988), Shyy and Udaykumar (1990), and Bloxsidge, Dowling, and Langhorne (1988). Furthermore, it provides a framework for the generalization of these models. Within this framework many possible forms of combustion response can be investigated.

4. Linear Stability Analysis

In this section a general linear stability analysis will be developed based on (5 a). The method of modal analysis will be used to accomplish this. Neglecting nonlinear terms in (5 a) and assuming

$$A = -\eta\phi - k\int\phi\, dt \tag{18}$$

(η and k being constants) yields

$$\frac{\partial^2\phi}{\partial t^2} - \frac{\partial^2\phi}{\partial x^2} + 2u_0\frac{\partial^2\phi}{\partial x\partial t} + \eta\frac{\partial\phi}{\partial t} + k\phi + (\gamma-1)Q = 0 \tag{19}$$

In (19) the terms multiplied by k and η play the roles of respective generic frequency change and damping effects not associated with either combustion or mean flow. They will subsequently be referred to as body force effects.

Let

$$\phi = \sum_{m=1}^{\infty} f_m(t)\,\psi_m(x) \tag{20}$$

where the ψ's are a complete set of orthonormal functions in the region $0 < x < 1$ satisfying

$$\psi_n'' + \Omega_n^2\psi_n = 0 \tag{21}$$

and the f's are the corresponding modal amplitudes. In (21) the Ω's are the natural frequencies of the associated acoustics problem (all terms except the first two neglected in (19)). Substituting (6) and (20) into (19), multiplying each term by $\psi_n(x)$, integrating from $x=0$ to $x=1$, noting that

$$\int_0^1 \psi_m(x)\psi_n(x)\,dx = \delta_{mn} \tag{22}$$

(orthonormality condition), and making the definitions

$$C_{mn} = \int_0^1 \psi_m'(x)\psi_n(x)\,dx, \qquad Q_n = \int_0^1 \bar{Q}(x)\,q(x,t)\,\psi_n(x)\,dx \tag{23}$$

yields

$$\ddot{f}_n + 2u_0\sum_{m=1}^{\infty} C_{mn}\dot{f}_m + \Omega_n^2 f_n + \eta\dot{f}_n + kf_n + (\gamma-1)Q_n = 0 \tag{24}$$

where a dot indicates time differentiation. Equation (23 b) must be evaluated separately for each of the two combustion models.

First, consider the local model which is characterized by the general equation

$$\mathcal{L}_1(q) = Y\mathcal{L}_2(u) = Y\mathcal{L}_2\left(\frac{\partial\phi}{\partial x}\right) \tag{25}$$

Substituting (20) and

$$q = \sum_{m=1}^{\infty} g_m(t)\,\psi_m'(x) \tag{26}$$

into (25) yields

$$\mathcal{L}_1(g_n) = Y\mathcal{L}_2(f_n) \tag{27}$$

Substituting (26) into (23 b) gives

$$Q_n = \sum_{m=1}^{\infty} D_{mn}\,g_m(t) \tag{28}$$

where

$$D_{mn} = \int_0^1 \bar{Q}(x)\,\psi_m'(x)\,\psi_n(x)dx \tag{29}$$

Second, consider the convection model which is characterized by the general equation

$$\mathcal{L}_1(q_s) = Y\mathcal{L}_2(u_s) = Y\mathcal{L}_2\left[\left(\frac{\partial\phi}{\partial x}\right)_s\right] \tag{30}$$

Substituting (20) and

$$q_s = \sum_{m=1}^{\infty} g_m(t)\,\psi_m'(x_s) \tag{31}$$

into (30) yields (27). Substituting (31) into (13) and substituting the result into (23 b) yields

$$Q_n = \sum_{m=1}^{\infty} \psi_m'(x_s)\int_{x_s}^{1} \bar{Q}(x)\,g_m\left(t-\frac{x-x_s}{V_c}\right)\psi_n(x)\,dx \tag{32}$$

Equation (24) was derived using an order of magnitude analysis which assumed that mean flow, combustion, and body forces produced small corrections to the associated acoustic response. This idea will also be used in the stability analysis to be presented next. The following discussion has much in common with the ideas of Culick (1988).

A first use of the small correction idea is to uncouple the modal amplitudes by assuming that the summations appearing in (24), (28), and (32) are dominated by the terms for which $m=n$. This reduces (24) to

$$\ddot{f}_n + \eta \dot{f}_n + (\Omega_n^2 + k) f_n + 2u_0 C_{nn} \dot{f}_n + (\gamma - 1) Q_n = 0 \tag{33}$$

Equations (27) and (33) form a determinate set of equations to solve for f_n and g_n.

Substituting the harmonic functions

$$f_n = \check{f}_n e^{i\omega_n t}, \qquad g_n = \check{g}_n e^{i\omega_n t} \tag{34}$$

into (27) (assuming constant Y) and substituting the result and (34 b) into the truncated forms of (28) and (32) yields

$$Q_n = \check{f}_n e^{i\omega_n t} Y I(\omega) D_{nn} \tag{35}$$

where

$$D_{nn} = \int_0^1 \bar{Q}(x)\, \psi_n'(x)\, \psi_n(x)\, dx \tag{36}$$

for the local model and

$$D_{nn} = \psi_n'(x_s) \int_{x_s}^1 \bar{Q}(x)\, e^{-i\omega_n\left(\frac{x - x_s}{v_c}\right)}\, \psi_n(x)\, dx \tag{37}$$

for the convection model. Substituting (34) and (35) into (33) yields the common form

$$\omega_n^2 - k - i(\eta + 2u_0 C_{nn})\omega_n - (\gamma - 1) Y D_{nn} I(\omega_n) = \Omega_n^2 \tag{38}$$

This algebraic equation must be solved to find the complex frequency ω_n.

A second use of the small correction idea is to solve (38) approximately as follows. It can be rewritten as

$$(\omega_n - \Omega_n)(\omega_n + \Omega_n) = k + i(\eta + 2u_0 C_{nn})\omega_n + (\gamma - 1) Y D_{nn} I(\omega_n) \tag{39}$$

A first approximation can then be obtained by neglecting the entire right hand side of (39) to yield

$$\omega_n = \pm \Omega_n \tag{40}$$

A second approximation can then be found by replacing ω_n in (39) by (40) everywhere except in the factor on the left hand side which would be reduced to zero by doing so. The result of doing this can be stated in a convenient form by first letting

$$\omega_n = \pm s_n + i\zeta_n \tag{41}$$

and noting that

$$e^{i\omega_n t} = e^{\pm i s_n t}\, e^{-\zeta_n t} \tag{42}$$

allows one to identify s_n as the frequency and ζ_n as the damping factor of the n'th mode. Then the second approximation can be written

$$s_n = s_{1,n} + s_{2,n} + s_{3,n}\,, \qquad \zeta_n = \zeta_{1,n} + \zeta_{2,n} + \zeta_{3,n} \tag{43}$$

where

$$s_{1,n} = \Omega_n \ , \qquad s_{2,n} = \frac{k}{2\Omega_n} \ , \qquad s_{3,n} = \frac{(\gamma-1)Y}{2\Omega_n}[D_{R,nn}I_R(\Omega_n) - D_{I,nn}I_I(\Omega_n)] \tag{44}$$

are the respective acoustic, body force, and combustion contributions to the frequency and

$$\zeta_{1,n} = u_0 C_{nn} \ , \qquad \zeta_{2,n} = \frac{\eta}{2} \ , \qquad \zeta_{3,n} = \frac{(\gamma-1)Y}{2\Omega_n}[D_{R,nn}I_I(\Omega_n) + D_{I,nn}I_R(\Omega_n)] \tag{45}$$

are the respective mean flow, body force, and combustion contributions to the damping factor.

The solution methodology employed herein automatically produces frequency and damping factor expressions which are sums of contributions due to individual effects. If a new physical effect is added, therefore, it is only necessary to determine its associated frequency and damping factor contributions and add them to those already existing. The entire solution need not be repeated.

It was possible to obtain (44) and (45) without specifying either the orthonormal functions $\psi_n(x)$ or the combustion impedance function $I(\omega_n)$. These results are, therefore, quite general and can be used under a variety of circumstances.

5. Applications

In this section, several examples of the application of the results of the previous section will be given. In these examples a simple time delay combustion model will be used. This is produced by allowing the operator $\mathcal{L}_1$ to take on the value unity and the operator $\mathcal{L}_2$ to produce a time delay τ. This yields the time domain form

$$q = Yu(t-\tau) \tag{46}$$

and the corresponding impedances

$$I_R(\omega) = \cos(\omega\tau) \ , \qquad I_I(\omega) = -\sin(\omega\tau) \tag{47}$$

Here τ is interpreted as a characteristic time associated with the combustion process. Concentrated steady heating rate and rectangular steady heating rate distributions will be investigated. Both the local and convection models are employed. Three combinations of boundary conditions (designated as open/open - O, closed/closed - C, and closed/open - M) are considered.

The concentrated steady heating rate distribution is expressed as

$$\bar{Q}(x) = \hat{Q}\Delta(x-\lambda) \tag{48}$$

where $\hat{Q}$ and λ are constants. Here the heating zone is idealized as a single cross section $x = \lambda$.

The respective acoustic frequencies and corresponding orthonormal eigenfunctions for various boundary conditions are shown in Table 1.

Table 1. Orthonormal eigenfunctions, circular frequencies for various boundary conditions.

	open/open (O)	closed/closed (C)	closed/open (M)
ψ_n	$\sqrt{2}\sin(n\pi x)$	$\sqrt{2}\cos(n\pi x)$	$\sqrt{2}\cos[\frac{(2n-1)\pi}{2}x]$
Ω_n	$n\pi$	$n\pi$	$\frac{(2n-1)\pi}{2}$

For the local model the combination of (36), (45c) and (48) results in

$$\zeta_n = \mp \frac{\gamma-1}{2}\hat{Q}Y_n \sin(2\Omega_n\lambda)\sin(\Omega_n\tau) \; ; \quad O(-), \;\; C,M(+) \qquad (49)$$

Equation (49) holds for all modes. The idealized nature of the steady heat release distribution (concentrated at one cross section) makes this expression relatively simple to interpret.

In most cases the behavior of the first mode is the most important in instability studies. For open/open or closed/closed conditions and a given mode number $n = 1$, (49) changes signs at $\lambda = 1/2$ and $\tau = 1$ provided the restriction of $0 < \tau < 2$. For open/open conditions, therefore, unsteady heating produces a tendency toward instability of the first mode for $\lambda < 1/2$ and $\tau < 1$ or $\lambda > 1/2$ and $\tau > 1$ and a tendency toward stability of the first mode otherwise. For closed/closed conditions, on the other hand, instability of the first mode is predicted for $\lambda > 1/2$ and $\tau < 1$ or $\lambda < 1/2$ and $\tau > 1$ and stability of the first mode is predicted otherwise.

For closed/open conditions it can be seen from (49) that the restriction $0 < \tau < 4$ can be imposed without loss of generality. Thus, ζ_1 is positive for all possible λ's and $\tau < 2$ and negative for all possible λ's and $\tau > 2$.

In all subsequent discussion, unless explicitly stated to the contrary, the behavior of ζ_1 (the first mode combustion damping factor) will be singled out for detailed discussion because of its importance in applications. It should be recalled, however, that the general damping factor expressions for ζ_n are correct for all modes.

Expression (49) is useful in explaining the behaviors of both the Rijke tube and jet engine augmentors. These issues will be discussed below.

First, consider the Rijke tube (see, for instance, Carrier (1955) or Culick (1970) and the references therein). In the Rijke tube a heater is located at an interior cross section of an open/open tube and subjected to mean flow. Under certain circumstances instability can occur. With the heater replaced by a combustion zone, this closely resembles the situation in certain types of ramjet combustion chambers. As mentioned previously, (49) shows that $\zeta_1 < 0$ is satisfied if $\lambda < 1/2$, provided that $\tau < 1$ (according to Carrier (1955) $\tau \approx 3/8$ for the Rijke tube). Therefore, the placement of the heating plane in the upstream half of the duct is predicted to result in excitation of the fundamental acoustic mode of the duct as is observed experimentally.

Next consider a highly simplified model of a turbofan augmentor. The augmentor is bounded on the upstream side by the turbine outlet and on the downstream side by a choked nozzle. Both of these boundaries are nearly acoustically closed. It is believed that the quality of fuel atomization and fuel droplet vaporization may be critical to stability. As the quality of these processes deteriorates, the combustion zone will move downstream in the augmentor. Assuming that the behavior is adequately described by the closed/closed boundary condition of (49), deterioration of atomization and vaporization could be roughly simulated by increasing λ. As mentioned previously, values of $\lambda > 1/2$ produce instability (provided that $\tau < 1$). This trend appears consistent with experimental observations.

For the convection interaction model the combination of (37), (45c) and (48) results in

$$\zeta_n = \begin{cases} -(\gamma-1)\hat{Q}Y_n\cos(\Omega_n x_s)\sin(\Omega_n\lambda)\sin[\Omega_n(\tau + \frac{\lambda - x_s}{u_c})] \; ; \; O \\ \\ (\gamma-1)\hat{Q}Y_n\sin(\Omega_n x_s)\cos(\Omega_n\lambda)\sin[\Omega_n(\tau + \frac{\lambda - x_s}{u_c})] \; ; \; C,M \end{cases} \qquad (50)$$

It can be seen that (50) can be reduced to (49) by making the substitution $x_s = \lambda$. Here the source cross section and the heating cross section have the same location which erases the distinction between the local and the convection interaction models. It can also be seen that the symmetry between the results for open/open and closed/closed ducts exhibited by the local interaction model is lost when the convection interaction model is employed.

The quantity $(\lambda - x_s)/u_c$ is the time required to travel the distance $\lambda - x_s$ separating the heating cross section from the source cross section at the convection velocity u_c. It can be seen that this quantity enters (50) as an additional effective phase shift. Since the parameters x_s, λ, τ, and u_c all appear in (50), it is helpful to put reasonable restrictions on as many of these parameters as possible as an aid to interpretation.

First, as mentioned in Section 3, the local flow velocity, the speed of sound, and the velocity of moving vortices have all been suggested as appropriate convection velocities. The local flow velocity is subsonic in ramjet and afterburner combustion chambers. The speed of moving vortices is likely to be of the order of the local flow velocity and, therefore, also subsonic. The dimensionless convection velocity is normalized with the undisturbed speed of sound and is the convection Mach number. Based on the considerations just discussed, it is reasonable to impose the restriction $0 \le u_c \le 1$. Second, it will be assumed that $0 \le \tau \le 1$. This is consistent with Carrier's (1955) estimate of $\tau \approx 3/8$. Third, it should be recalled that the geometry of the system imposes certain constraints. Thus, $0 \le x_s \le \lambda \le 1$ ($\Rightarrow \lambda - x_s \le 1$).

Inspection of (50) shows that reducing the convection velocity u_c with the other variables held fixed amplifies the influence of the values of λ and x_s. This indicates that relatively small changes in the operating conditions or geometry can have a large effect on stability. This is consistent with combustor observations.

Various phenomena can move the position of the combustion plane in an augmentor. This effect can be simulated in the present model by varying λ with other variables fixed. In the following discussion it will initially be assumed that $x_s < 1/2$.

Equation (50) shows that for the open/open configuration ζ_1 will be negative for sufficiently small values of λ and may become positive as λ increases. This is qualitatively similar to the behavior exhibited by (49). According to (49) there is only one sign change which occurs at $\lambda = 1/2$. According to (50), on the other hand, the first sign change will occur at $\lambda_1 = x_s + (1-\tau)u_c$ provided that $\lambda_1 < 1$. If $\lambda_1 > 1$, there will be no stable operation. A total of M sign changes in ζ_1 will occur at the values $\lambda_m = x_s + (m-\tau)u_c$; $m = 1, 2, \cdots, M$ with M being the lowest integer for which $\lambda_{M+1} > 1$. It can be seen that low values of u_c will correspond to many sign changes in consistency with the previous discussion of the influence of u_c. All the signs discussed above will be reversed for $x_s > 1/2$.

Inspection of (50) reveals that for the closed/closed case sufficiently small values of λ correspond to stable behavior of the first mode ($\zeta_1 > 0$) and that increasing λ will lead to unstable behavior. This is qualitatively consistent with (49). The first sign change will occur at the smaller of $\lambda = 1/2$ and $\lambda_1 = x_s + (1-\tau)u_c$. If $\lambda_1 > 1$ there will be one sign change in ζ_1 at $\lambda = \lambda_\ell$. If $\lambda_1 < 1$ there will be $1 + M$ sign changes at $\lambda = \lambda_\ell$, λ_m with λ_m and M be defined as in the previous paragraph. The signs discussed in this paragraph will not be affected by the value of x_s.

The expression for ζ_1 given by (50) for the closed/open geometry will be positive for sufficiently small λ. This is qualitatively consistent with (49) which indicates stability for all λ. A change to unstable behavior will occur at $\lambda = \lambda_2$ (provided $\lambda_2 < 1$). Additional sign changes will occur at $\lambda = \lambda_4, \lambda_6, \cdots$ as long as these λ's are less than unity. Reducing u_c will increase the number of λ's satisfying this criterion. The value of x_s will not affect the signs discussed above.

The possibility of a large number of sign changes in ζ_1 with increasing λ is one feature which clearly distinguishes the convection interaction model from the local interaction model. This property can be used in an analysis of experimental results to help decide which model best describes them.

Varying x_s with $\lambda - x_s$ and u_c held fixed in the present model provides a simplistic simulation of changing the flameholder position in an augmentor. It should be recalled that increasing x_s automatically increases λ in this case. The effective time delay $\tau_e = \tau + (\lambda - x_s) / u_c$ is not changed by this type of parametric change.

Equation (50) indicates a transition from unstable to stable behavior of the first mode at $x_s = 1/2$ for the open/open case. Since moving the source downstream automatically moves the heating plane downstream, it can be said that this behavior is qualitatively similar to that predicted by the local model (see (49)).

For the closed/closed case (50) shows that ζ_1 exhibits a change from positive to negative at $\lambda = 1/2$. For a situation in which λ is initially less than $1/2$, increasing x_s increases λ and eventually produces unstable behavior. This is qualitatively similar to the behavior predicted for the local interaction model by (49). If λ is initially greater than $1/2$, unstable behavior will exist for all flameholder positions.

For the closed/open configuration (50) indicates stable behavior for all source (and, thus, all heating) cross section locations. This is qualitatively similar to the prediction of (49) for the local model.

It can be seen from the previous discussion that there is considerable qualitative similarity between the predictions of the local and convection models.

The rectangular steady heating rate distribution is expressed as

$$\bar{Q}(x) = Q_0[H(x - \lambda_1) - H(x - \lambda_2)] \tag{51}$$

where Q_0, λ_1, and λ_2 are constants. Here the heating zone is the region $\lambda_1 < x < \lambda_2$ and the steady heating rate is assumed to be uniform therein.

For the local model, the combination of (36), (45c) and (51) produces

$$\zeta_n = \mp \frac{\gamma - 1}{2\Omega_n} Q_0 Y_n \sin[\Omega_n(\lambda_2 - \lambda_1)] \sin[\Omega_n(\lambda_2 + \lambda_1)] \sin(\Omega_n \tau) \ ; \ O(-), \ C,M(+) \tag{52}$$

For open/open conditions, (52) indicates that the first mode will be unstable for $\lambda_1 + \lambda_2 < 1$ (or $(\lambda_1 + \lambda_2)/2 < 1/2$). The quantity $(\lambda_1 + \lambda_2)/2$ is the location of the center of the heating zone. This condition requires that the center of the heating zone be in the upstream half of the duct (thus generalizing Rijke's result). For closed/closed conditions, the first mode will be unstable for $\lambda_1 + \lambda_2 > 1$. This condition requires that the center of the heating zone be in the downstream half of the duct. For closed/open conditions, ζ_1 is positive for all possible locations of the center of the heating zone. These results are qualitatively similar to those for the concentrated heating distribution. It can be seen that the magnitudes of the damping factors decrease with mode number for the rectangular heating distribution while this is not observed for the concentrated heating distribution.

It is interesting to note that the solutions for open/open and closed/closed conditions are identical except the sign, which is also observed in the local model of concentrated heating. In fact, (48) is a special case of (51) which is readily demonstrated by substituting

$$Q_0 = \frac{\hat{Q}}{\lambda_2 - \lambda_1} \tag{53}$$

into (51) and taking the limit as $\lambda_2 \to \lambda_1 = \lambda$ to get (48). It is clear that the value of τ will affect the sign of ζ_1.

For the convection model it is necessary to state the results of combining (37) and (45c) with (51) in two separate forms. For $u_c \neq 1$ it is found that

$$
\zeta_n = \begin{cases}
\dfrac{(\gamma-1)u_c}{\Omega_n(1-u_c)(1+u_c)} Q_0 Y_n \cos(\Omega_n x_s) \cdot \\
\cdot \left\{ (1-u_c)\cos\left(\Omega_n [\tau + (\dfrac{1+u_c}{u_c}\dfrac{\lambda_2+\lambda_1}{2} - \dfrac{x_s}{u_c})] \right) \sin(\Omega_n \dfrac{1+u_c}{u_c}\dfrac{\lambda_2-\lambda_1}{2}) \right. \\
\left. - (1+u_c)\cos\left(\Omega_n [\tau + (\dfrac{1-u_c}{u_c}\dfrac{\lambda_2+\lambda_1}{2} - \dfrac{x_s}{u_c})] \right) \sin(\Omega_n \dfrac{1-u_c}{u_c}\dfrac{\lambda_2-\lambda_1}{2}) \right\} ; \ O \\
\dfrac{(\gamma-1)u_c}{\Omega_n(1-u_c)(1+u_c)} Q_0 Y_n \sin(\Omega_n x_s) \cdot \\
\cdot \left\{ (1-u_c)\sin\left(\Omega_n [\tau + (\dfrac{1+u_c}{u_c}\dfrac{\lambda_2+\lambda_1}{2} - \dfrac{x_s}{u_c})] \right) \sin(\Omega_n \dfrac{1+u_c}{u_c}\dfrac{\lambda_2-\lambda_1}{2}) \right. \\
\left. + (1+u_c)\sin\left(\Omega_n [\tau + (\dfrac{1-u_c}{u_c}\dfrac{\lambda_2+\lambda_1}{2} - \dfrac{x_s}{u_c})] \right) \sin(\Omega_n \dfrac{1-u_c}{u_c}\dfrac{\lambda_2-\lambda_1}{2}) \right\} ; \ C, M
\end{cases} \tag{54}
$$

Inspection of (54) shows an indeterminacy at $u_c = 1$. Thus a separate expression is needed for $u_c = 1$ which is

$$
\zeta_n = \begin{cases}
\dfrac{\gamma-1}{2} Q_0 Y_n \cos(\Omega_n x_s) \cdot \\
\cdot \left\{ \dfrac{1}{\Omega_n} \sin[\Omega_n(\lambda_2-\lambda_1)] \cos[\Omega_n(\tau+\lambda_2+\lambda_1-x_s)] - (\lambda_2-\lambda_1)\cos[\Omega_n(\tau-x_s)] \right\} ; \ O \\
\dfrac{\gamma-1}{2} Q_0 Y_n \sin(\Omega_n x_s) \cdot \\
\cdot \left\{ \dfrac{1}{\Omega_n} \sin[\Omega_n(\lambda_2-\lambda_1)] \sin[\Omega_n(\tau+\lambda_2+\lambda_1-x_s)] + (\lambda_2-\lambda_1)\sin[\Omega_n(\tau-x_s)] \right\} ; \ C, M
\end{cases} \tag{55}
$$

Equations (54) and (55) appear too complicated to be interpreted by inspection. Therefore, a few representative sets of numerical results will be presented to illustrate important trends. In the following discussion the open/open case is selected as representative and attention is limited to the first mode. On each figure, a corresponding case of concentrated heating is shown for comparison. The correspondence is established by equating the center of the rectangular heating distribution, $(\lambda_1 + \lambda_2)/2$, to the position of the concentrated heating cross section, λ. Equation (53) is used to insure the same steady heating rate in both cases.

Figure 1 illustrates the influence of the convection velocity u_c on the damping factor ζ_1 for open/open conditions and response model 1. It can be seen that reductions in the convection velocity lead to more and more rapid oscillations in the sign of ζ_1. This is true for both concentrated and rectangular heating distributions. It is interesting to note, however, that while the magnitude of ζ_1 approaches zero as u_c approaches zero for the rectangular cases, it remains finite for the concentrated case.

It should be kept in mind when viewing Figure 1 and similar subsequent figures that ζ_1 is directly proportional to the quantities Y, Q_0 (or $\hat{Q}$), and $\gamma - 1$. Thus results obtained for representative values of these quantities can be readily extended to other parametric combinations by simple multiplication.

Figure 2 demonstrates the influence of varying the center of the heating zone $\lambda = (\lambda_1 + \lambda_2)/2$ on the damping factor ζ_1. For the concentrated heating distribution it can be seen, as discussed earlier, that moving the heating cross section sufficiently far downstream produces stability. The same trend is observed for rectangular heating distributions with one important difference. The system geometry requires that the inequality

$$\frac{\lambda_2 - \lambda_1}{2} \leq \lambda \leq 1 - \frac{\lambda_2 - \lambda_1}{2} \tag{56}$$

must be satisfied. Thus increases in the width of the heating zone decrease the range of physically possible center positions. This is reflected in Figure 2. For the largest widths it is not possible to move the center of the heating zone sufficiently far downstream to produce stability. This is a qualitative difference between the concentrated and rectangular heating distributions.

When the quality of the fuel atomization and/or droplet vaporization processes in a combustor decreases, the heating zone moves downstream. Then, it is possible that part of the potential heating zone is pushed out the end of the chamber and some fuel escapes unburned into the nozzle. Figure 3 illustrates the influence of varying the center of the heating zone $\lambda = (\lambda_1 + \lambda_2)/2$ until the left end of the heating zone λ_1 meets the right end of the duct. As mentioned earlier, moving the heating zone sufficiently far downstream produces a tendency toward stability. This is augmented in the present case by the fact that less than 100 percent of the potential heating zone is realized for $\lambda > 0.7$.

Figure 4 illustrates the influence of changing the source position x_s with $\lambda - x_s$ held fixed. It can be seen that there is a sign change of ζ_1 from negative to positive at $x_s = 1/2$. Here the system geometry requires the satisfaction of the inequalities

$$0 \leq x_s \leq 1 - (\lambda - x_s + \frac{\lambda_2 - \lambda_1}{2}) , \quad 0 \leq \lambda_2 - \lambda_1 \leq 2(\lambda - x_s) \tag{57}$$

As discussed earlier in a different context, for the large heating zone lengths it is not possible to achieve stability in this configuration.

In general, the behaviors associated with concentrated heating distribution and the rectangular heating distribution are qualitatively similar. There are, however, some important differences as discussed above.

6. Conclusion

In this paper a general formulation of the problem of longitudinal combustion instability in ramjets and afterburners was given. A single wave equation governing a velocity potential was derived which can be used for both linear and nonlinear combustion instability predictions. A comprehensive linear velocity sensitive combustion model was developed which included several previous models as special cases. A modal analysis was carried out for linear problems. Based on this, a general linear stability analysis was performed. Finally, several examples of the application of this stability analysis were discussed.

References

[1] Bloxsidge, G.J., Dowling, A.P., and Langhorne, P.J., 1988, "Reheat buzz: an acoustically coupled combustion instability. Part 2. Theory," *Journal of Fluid Mechanics*, Vol. 193, pp. 445-473.

[2] Carrier, G.F., 1955, "The Mechanics of the Rijke Tube," *Quarterly of Applied Mathematics*, Vol. 12, No. 4, pp. 383-395.

[3] Culick, F.E.C., 1970, "Stability of Longitudinal Oscillations with Pressure and Velocity Coupling in a Solid Propellant Rocket," *Combustion Science and Technology*, Vol. 2, pp.

179-201.

[4] Culick, F.E.C., 1988, "Combustion Instabilities in Liquid-Fueled Propulsion Systems - An Overview," *AGARD Conference Proceedings* - 450.

[5] Langhorne, P.J., 1988, "Reheat buzz: an acoustically coupled combustion instability. Part 1. Experiment," *Journal of Fluid Mechanics*, Vol. 193, pp. 417-443.

[6] Shyy, W. and Udaykumar, H., 1990, "Numerical Simulation of Thermo-Acoustic Effect on Longitudinal Combustion Instabilities," *A Paper AIAA 90-2065, Presented at the 26th Joint Propulsion Conference*, Orlando, Florida.

[7] Strutt, J.W. (Lord Rayleigh), 1945, *The Theory of Sound*, Vol.2, Dover Publications, New York.

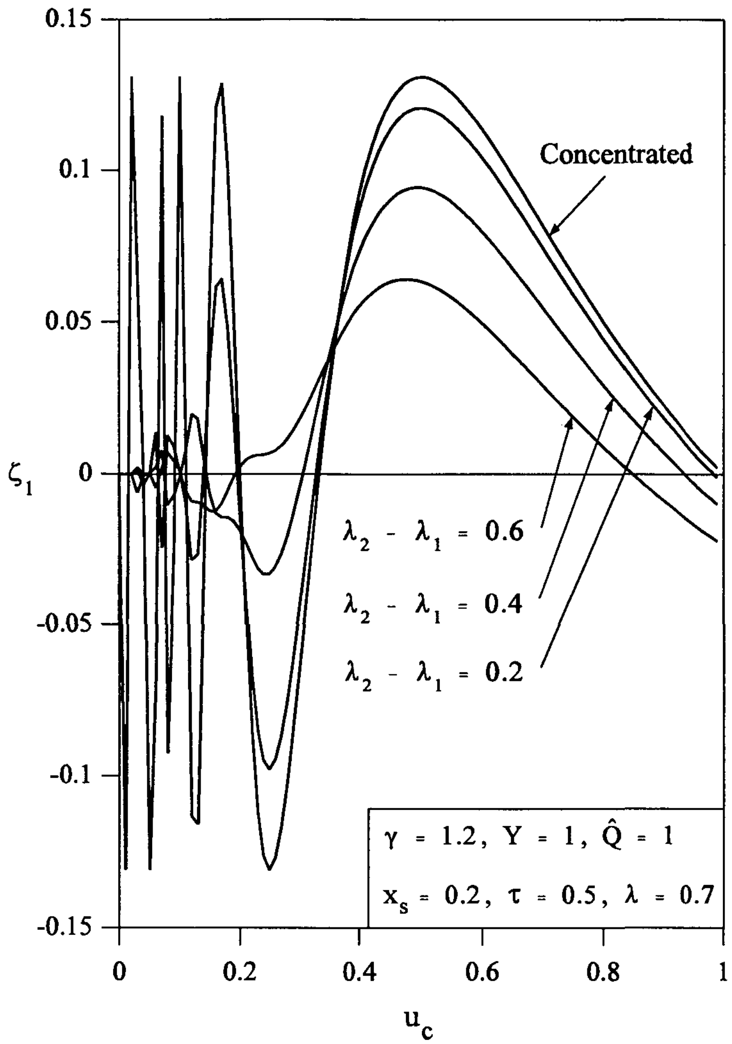

Fig. 1. Damping factor vs. convection speed for rectangular steady heating (O,convection response model).

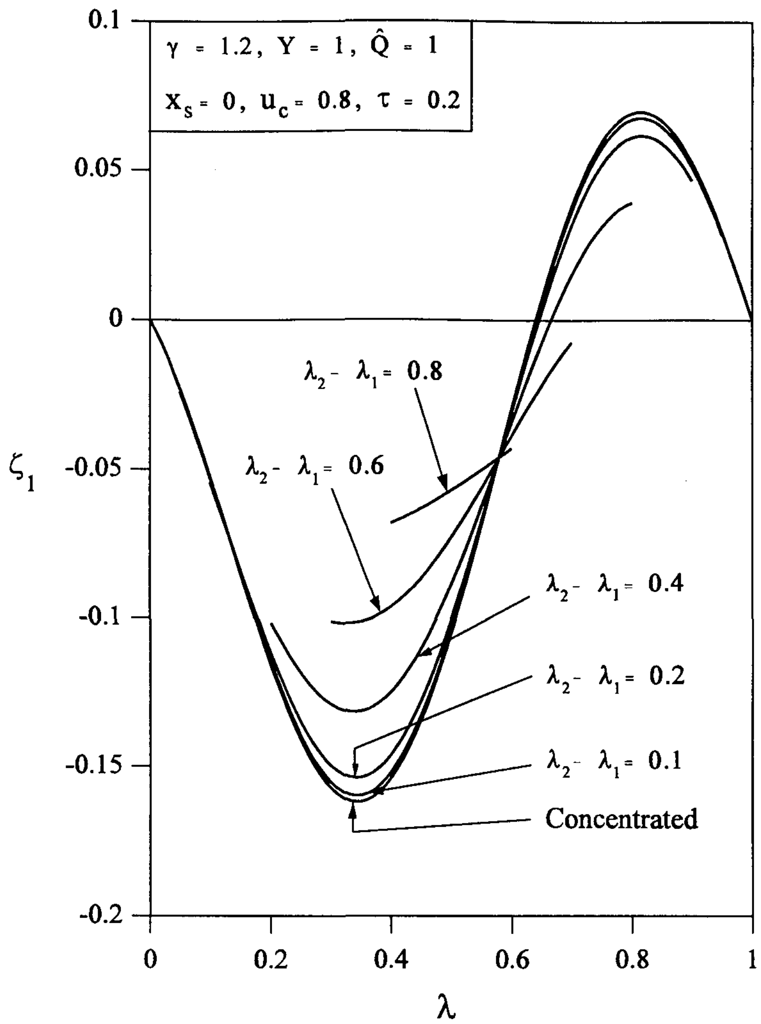

Fig. 2. Damping factor vs. center of the heating zone for rectangular steady heating (O, convection response model).

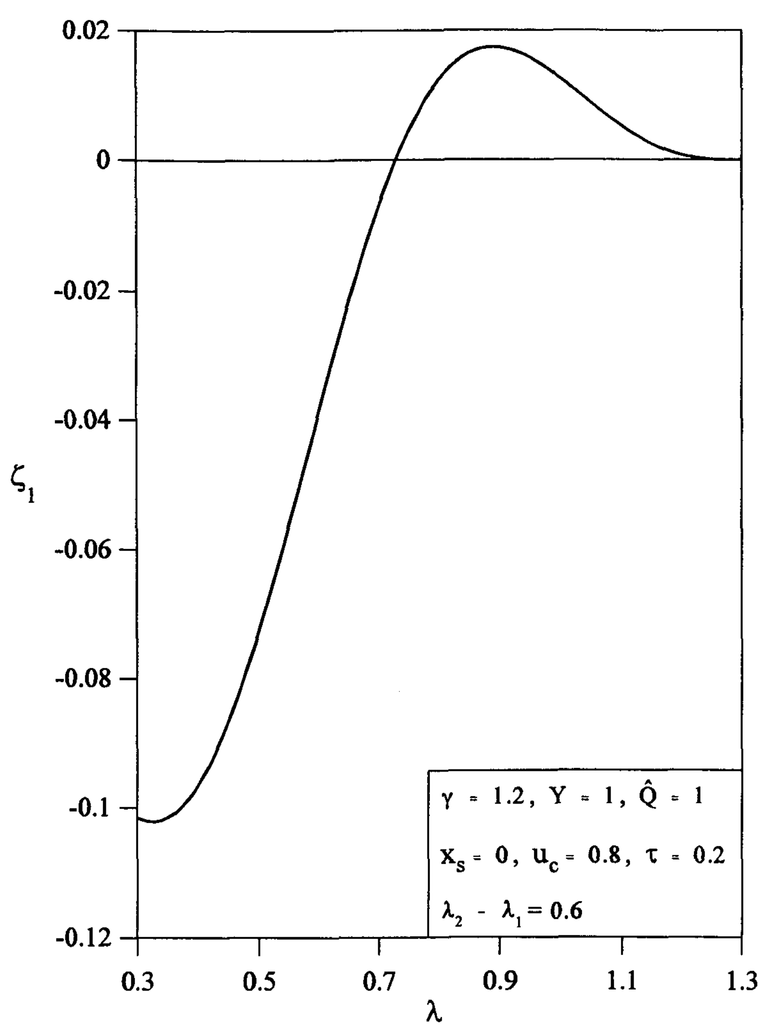

Fig. 3. Damping factor vs. center of the heating zone for rectangular steady heating (O, convection response model).

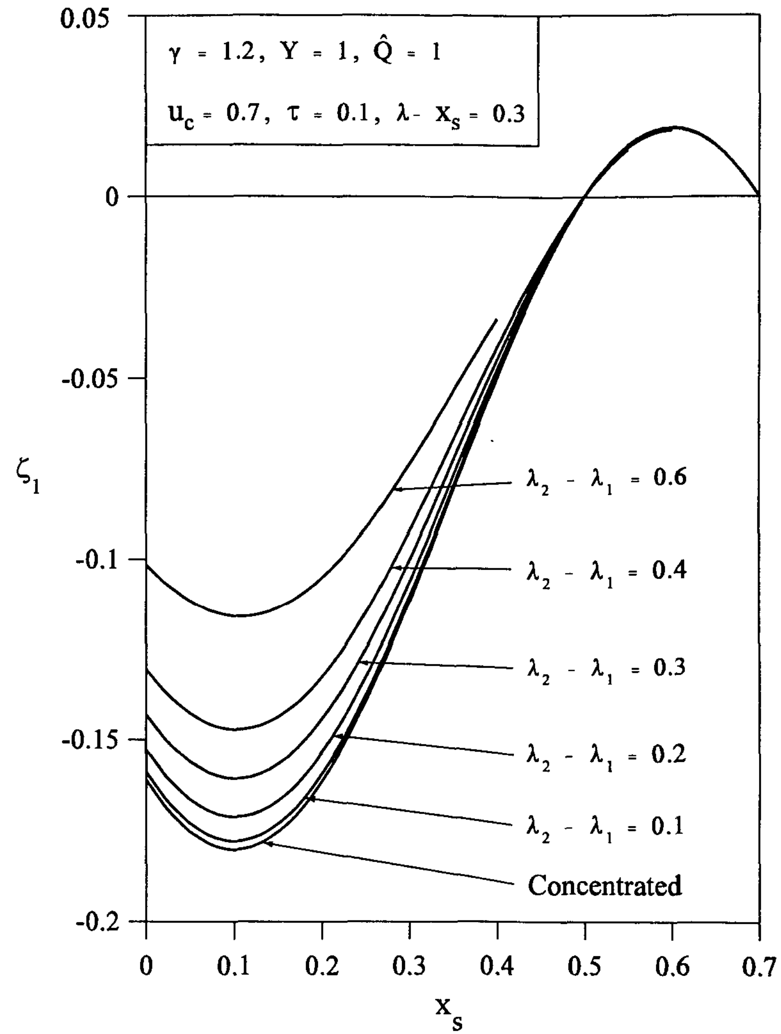

Fig. 4. Damping factor vs. source position for rectangular steady heating (O, convection response model).